AIP | Applied Physics Letters

Polymer photodetector with voltage-adjustable photocurrent spectrum

En-Chen Chen, Chia-Yu Chang, Ji-Ting Shieh, Shin-Rong Tseng, Hsin-Fei Meng, Chain-Shu Hsu, and Sheng-Fu Horng

Citation: Applied Physics Letters **96**, 043507 (2010); doi: 10.1063/1.3284648
View online: http://dx.doi.org/10.1063/1.3284648
View Table of Contents: http://scitation.aip.org/content/aip/journal/apl/96/4?ver=pdfcov
Published by the AIP Publishing

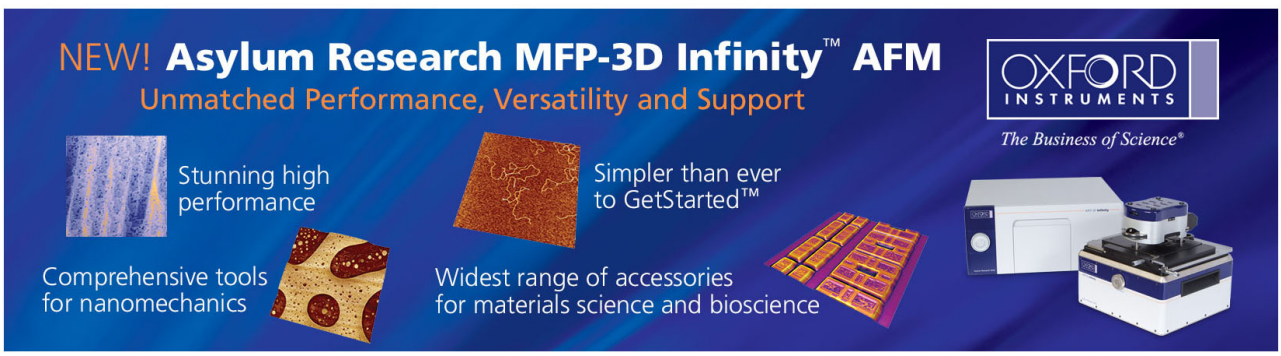

Polymer photodetector with voltage-adjustable photocurrent spectrum

En-Chen Chen,[1] Chia-Yu Chang,[2] Ji-Ting Shieh,[1] Shin-Rong Tseng,[3] Hsin-Fei Meng,[2,a)] Chain-Shu Hsu,[3] and Sheng-Fu Horng[1]
[1]*Institute of Electronics Engineering, National Tsing Hua University, Hsinchu 300, Taiwan*
[2]*Institute of Physics, National Chiao Tung University, Hsinchu 300, Taiwan*
[3]*Department of Applied Chemistry, National Chiao Tung University, Hsinchu 300, Taiwan*

(Received 22 June 2009; accepted 12 December 2009; published online 29 January 2010)

Polymer photodetectors with voltage-adjustable photoresponse from visible to near infrared range are demonstrated. Poly(3-hexylthiophene) and (6,6)-phenyl-C61-butyric acid methyl ester (PCBM) blend is used as the active layer. The photoresponse can be continuously adjusted by the thickness of the active layer as well as the applied voltage bias. The thickness of the active layer is varied from 250 nm to 16.2 μm. The mechanism for the photoresponse adjusted by the thickness can be attributed to the absorption of the photons in the infrared range by thick PCBM layer. The mechanism for the photoresponse adjusted by the applied bias can be attributed to the carrier recombination reduction when the applied bias increases. The adjustable photodetector also has high operating speed up to 10 kHz. © *2010 American Institute of Physics*. [doi:10.1063/1.3284648]

Organic photodetectors based on conjugated polymers have been the subject of extensive research in the last decades due to several inherent advantages as follows: low cost fabrication, high density large-area array, and the potentials for flexible applications.[1] Polymer photodetectors have high potential especially for signal processing and optical sensing systems.[2,3] In general the photoresponse of photodetectors is determined by the absorption of the active layer. The absorption of the active layer is relative to the band gap of materials. Most conjugated polymers have the response in the visible range due to the fact that the band gap of most organic semiconductor is higher than 2 eV. Low band-gap polymers are synthesized for infrared range response.[4–9] Therefore, specific materials are chosen for different photoresponses. However, it is difficult to fabricate photodetectors with patterned two or more specific materials for high density array by solution process. There will be many interesting imaging applications, if the response spectra can be switched by the voltage between visible and infrared ranges. So far there is no report of photodetectors with adjustable photoresponse from the same active layer. In this work a donor-acceptor blend, poly(3-hexylthiophene) (P3HT) and (6,6)-phenyl-C61-butyric acid methyl ester (PCBM), is used to be the active layer of the photodetector with adjustable response range. The thickness of the active layer is chosen to be greater than the visible photon penetration depth but comparable to the infrared photon penetration depth. P3HT:PCBM blend is commonly used in polymer solar cells and polymer photodetectors.[10] Both the P3HT and PCBM have photoresponses in visible range. In the previous letter, we studied the feasibility of P3HT:PCBM for the infrared photodetector.[11] The results showed that the photoresponse could be changed from visible to infrared by simply increasing the thickness of the active layer. We indicated the infrared absorption from so-called "charge-transfer exciton."[12,13] For this further study, we find the photoresponse can be continuously adjusted by the operating voltages. We continuously change the thickness of active layer from 250 nm to 16.2 μm. The photoresponse can be continuously adjusted from visible range to near infrared range. Particularly in the photodetector with 8.3 μm active layer the photoresponse starts in near infrared range under low reverse bias about 10 V and then extends to visible range, while the reverse bias increases to 100 V. The origin of this remarkable voltage dependence of the response spectrum is related to the electron-hole recombination of the visible light photons in the films much thicker than the penetration depth. The visible photons are absorbed near the transparent electrode where a high density of dark carriers are presented due to the diffusion from the metal contact.[16] There is, therefore, high probability of recombination before the collection by the other electrode at low voltages. At high reverse bias voltages the dark carrier density is lower and the carrier moves faster so the recombination is reduced and collection efficiency increases. On the other hand the infrared photons have a penetration depth comparable to the film thickness and the carriers are generated away from the dark carriers near the metal contact, so the collection by the electrodes is easier regardless of the voltage. Numerical simulations on the recombination rates and photocurrents are used to support this picture.

The devices are fabricated with similar process described in previous report.[11] The devices of active layer with thickness of 250 and 710 nm are formed by spin coating. The devices with thicker active layers with thickness of 4.1, 8.3, and 16.2 μm are formed by drop casting. The external quantum efficiency (EQE) is measured by the spectral response measurement system (SR300, Optosolar GMBH). The morphology of P3HT:PCBM is monitored by atomic force microscope (AFM) (Dimension 3100, Digital Instruments). The scale bar is 100 nm. For the transient response measurement, inorganic light-emitting diode (LED) with 650 nm emission is driven by a function generator. The photocurrent of polymer photodetector is amplified by transimpedance amplifier (DHPCA-100, Femto-tech Inc.) and the output signal is read from digital oscilloscope. In addition, we verify the idea by theoretical calculation with the model based on our previous letters on organic LEDs and organic photovoltaics.[14–16]

a)Author to whom correspondence should be addressed. Electronic mail: meng@mail.nctu.edu.tw.

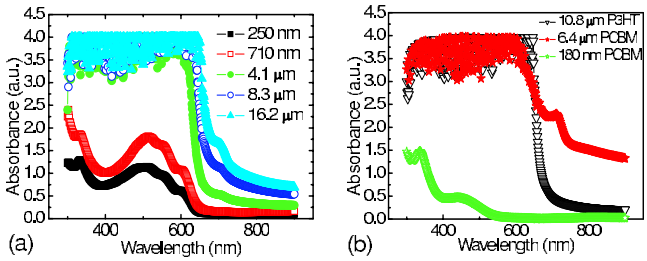

FIG. 1. (Color online) The absorption of (a) P3HT:PCBM layer with thickness of 250 nm (solid square), 710 nm (empty square), 4.1 μm (solid circle), 8.3 μm (empty circle), and 16.2 μm (solid triangle). (b) 10.8 μm P3HT layer (empty triangle), 6.4 μm PCBM layer (solid star), and 180 nm PCBM (empty star).

The absorption spectra of the P3HT:PCBM films with different thicknesses are shown in Fig. 1(a). As can be seen most visible light can be absorbed by all the devices with different thicknesses. The differences of the absorption can be observed in the near infrared range (650 to 1000 nm). The absorption intensity in the infrared range increases with the film thickness increase. In order to further study the origin of the infrared absorption, the absorption spectra of thick pure P3HT and PCBM layer are measured, shown in Fig. 1(b). Obviously the absorption in infrared range of PCBM layer increases dramatically when the thickness of PCBM increases to 6.4 μm. There is no absorption in infrared range of P3HT layer even with the film thickness of 10.8 μm. This should be the main mechanism of the previous letter about using P3HT:PCBM blend for infrared detection.[3] The P3HT in the active layer is just used to create the heterojunction for exciton dissociation and charge transport. Figure 2 shows the EQE of the photodetectors with different thicknesses. The

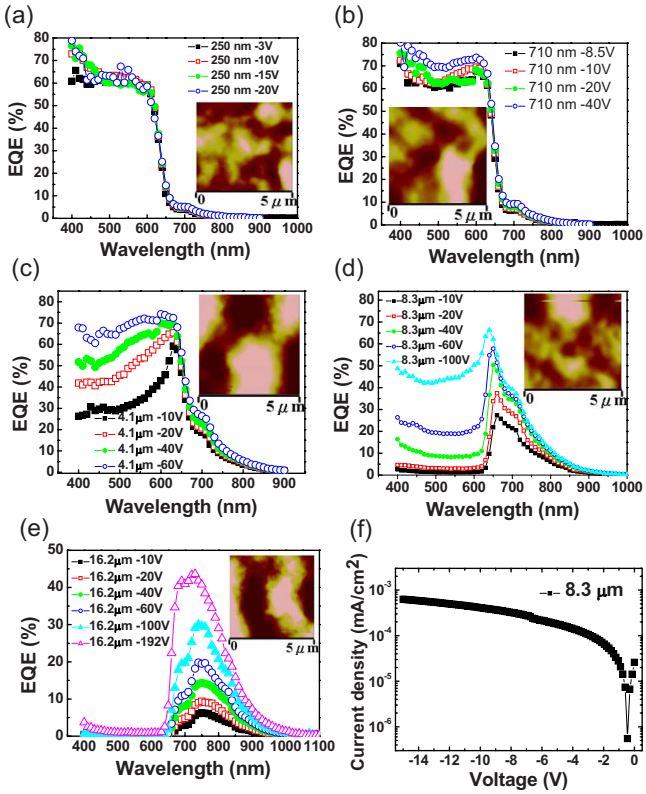

FIG. 2. (Color online) EQE and AFM images of the devices with different thicknesses (a) 250 nm, (b) 710 nm, (c) 4.1 μm, (d) 8.3 μm, and (e) 16.2 μm. (f) Dark current density of 8.3 μm devices.

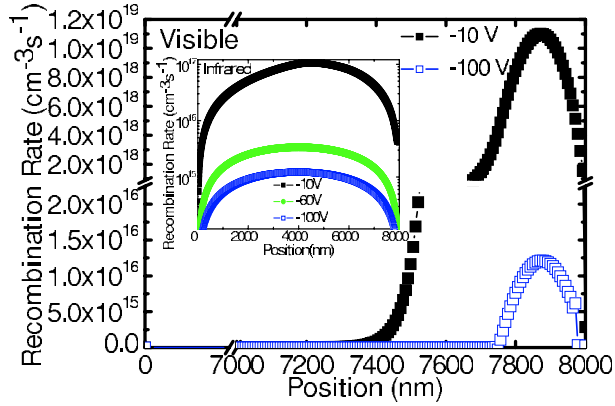

FIG. 3. (Color online) Calculated recombination rate in the 8 μm device in the visible range. The calculated recombination rate in the infrared range is shown in the inset.

EQE values of the devices with 250 and 710 nm active layers are about 60% to 70% in visible range and 5% to 10% in near infrared range (wavelength of 700 nm) under the reverse biases. As the thickness of active layer increases to 4.1 μm, the EQE value in visible range decreases to 30%–50% under the reverse bias of 10 V, and increases to 70% when the reverse bias increases to 60 V. The EQE value in the near infrared range increases to 25% at 700 nm. As the thickness of the active layer increases to 8.3 μm, the EQE value decreases to almost zero in the visible range under the reverse bias of 10 V. The EQE value of the 8.3 μm device in visible range increases to about 50% when the reverse bias increases to 100 V. Interestingly the EQE value in the infrared range increases from 20% to 40% at 700 nm when the reverse bias increases from 10 to 100 V. Such result shows that the photoresponse can be adjusted by the applied voltages. When the thickness of the active layer increases to 16.2 μm, the photoresponse is only in the infrared range. The EQE value of the 16.2 μm device increases from 6% to 40% when the reverse bias increases from 10 to 192 V. Figure 2(f) shows the dark current density of the 8.3 μm device. The main mechanism for the photoresponse change can be described by visible and infrared parts individually. The absorption in visible range comes from the P3HT, and most photons in the visible range are absorbed within the thickness of 200 nm, resulting in high EQE values of the 250 and 710 nm devices. While the thickness increases most absorption occurs to generate excitons near the interface between the PEDOT:PSS and active layer. It is difficult for the carriers dissociated from the excitons to go across the bulk and be collected by the cathode to generate photocurrent. Most carriers recombine with each other again in the bulk thus reducing the EQE in the visible range when the thickness increases. On the other hand, the photons in the infrared range can be absorbed by the thick PCBM, therefore the EQE value increases when the active layer thickness increases. The AFM images for the thick drop-cast P3HT:PCBM film and thin spin-coated film are added in Fig. 2. There is no clear difference in the morphologies. The adjustable infrared photocurrent spectrum of the thick films is, therefore, completely due to the high thickness comparable to the penetration depth of the infrared photon. The absorption of the photons in the infrared range occurs within all the bulk of active layer, thus generating excitons in all the bulk. It is easier for the carriers from the photons in the infrared range to be

TABLE I. Calculated total currents and recombination currents of 250 nm and 8 μm devices.

Device	Voltage (V)	J_{total} (mA/cm^2)	J_{recomb} (mA/cm^2)
Visible range, thickness=250 nm	−10	4.1×10^{-3}	4.1×10^{-10}
Visible range, thickness=8 μm	−10	1.8×10^{-9}	3.6×10^{-5}
	−100	3.9×10^{-4}	3.1×10^{-8}
Infrared range, thickness=8 μm	−10	3.1×10^{-3}	9.5×10^{-3}
	−100	2×10^{-2}	9.5×10^{-4}

collected by the electrode due to the shorter distance for the carriers to be collected by the electrodes.

In order to verify the mechanism theoretical calculation of the device with 8 μm active layer is performed. Here we assume the carrier generation in the visible range occurs within 250 nm from the interface between active layer and PEDOT:PSS layer and the exciton generation in the infrared range within all the bulk. We also assume the generation rate in the visible range is the same as that in the infrared range (1×10^{-20} cm^{-3} s^{-1}). The model and relative factors are described in the previous letter.[16] Figure 3 shows the recombination rate of the carriers in the bulk. As can be seen the recombination rate decreases dramatically both in visible and infrared range when the reverse bias increases, indicating that more carriers can be collected by the electrodes and photocurrents will increase. The total current density (J_{total}) and recombination current density (J_{recomb}) in visible and infrared range are shown in Table I. For the visible range the J_{total} and J_{recomb} of the 250 nm device are 4.1×10^{-3} and 4.1×10^{-10} mA/cm^2, respectively, under the reverse bias of 10 V. The J_{total} reduces to 1.8×10^{-9} mA/cm^2 and the J_{recomb} increases to 3.6×10^{-5} mA/cm^2 due to the large carrier recombination when the thickness increases to 8 μm. The J_{total} increases to 3.9×10^{-4} mA/cm^2 and the J_{recomb} decreases to 3.1×10^{-8} mA/cm^2 when the bias increases to 100 V, thus enhancing carrier collection and the EQE. As to infrared range, the J_{total} and J_{recomb} are 3.1×10^{-3} and 9.5×10^{-3} mA/cm^2, respectively, under the reverse bias of 10 V. The J_{total} increases to 2×10^{-2} mA/cm^2 and the J_{recomb} decreases to 9.5×10^{-4} mA/cm^2 when the bias increases to 100 V. The calculation result supports the mechanism of the absorption change in visible and infrared range when the applied bias increases.

In addition to the sensitivity, fast response is an important issue of photodetector for the application of the high-speed scanning in the large area photodetector array. The frame rate of photodetector array is limited by the speed of photodetector. Figure 4 shows the results of the photocurrent response of the 8.3 μm device. As can be seen the photocurrent responses of both devices show a saturation at 20 Hz but become triangular shape at 10 kHz. The carrier mobility of 10 kHz operation could be estimated about 10^{-5} cm^2/V s by calculating the average drift velocity under the assumption of the uniform electric field in the active layer.

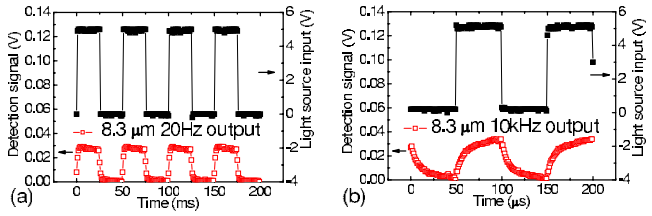

FIG. 4. (Color online) Transient response of the photodetector with 8.3 μm active layer under (a) 20 Hz and (b) 10 kHz.

In summary, photodetectors based on P3HT and PCBM blend with adjustable photoresponse and high operation speed are fabricated. The photoresponse can be adjusted from visible to infrared range by simply tuning the active layer thickness and applied bias. The mechanisms have been attributed to the absorption change from PCBM thickness change combined with carrier recombination change from the applied bias, which has been verified by the theoretical calculation. Such photodetectors provide many applications for different detection ranges. There is no need to fabricate patterned photodetectors with different materials for different response ranges.

This work is supported by the National Science Council of Taiwan under Grant Nos. NSC97-2628-M-009-016 and NSC97-2120-M-007-004.

[1]H. Y. Chen, M. K. F. Lo, G. Yang, H. G. Monbouquette, and Y. Yang, Nat. Nanotechnol. **3**, 543 (2008).
[2]Y. Ohmori, H. Kajii, M. Kaneko, K. Yoshino, M. Ozaki, A. Fujii, M. Hikita, and H. Takenaka, IEEE J. Sel. Top. Quantum Electron. **10**, 70 (2004).
[3]E. C. Chen, S. R. Tseng, J. H. Ju, C. M. Yang, H. F. Meng, S. F. Horng, and C. F. Shu, Appl. Phys. Lett. **93**, 063304 (2008).
[4]E. Perzon, X. Wang, F. Zhang, W. Mammo, J. L. D. P. D. L. Cruz, O. Inganäs, F. Langa, and M. R. Andersson, Synth. Met. **154**, 53 (2005).
[5]E. Perzon, X. Wang, S. Admassie, O. Inganäs, and M. R. Andersson, Polymer **47**, 4261 (2006).
[6]M. H. Petersen, O. Hagemann, K. T. Nielsen, M. Jorgensen, and F. C. Krebs, Sol. Energy Mater. Sol. Cells **91**, 996 (2007).
[7]L. Wen, B. C. Duck, P. C. Dastoor, and S. C. Rasmussen, Macromolecules **41**, 4576 (2008).
[8]J. Hou, H. Y. Chen, S. Zhang, G. Li, and Y. Yang, J. Am. Chem. Soc. **130**, 16144 (2008).
[9]X. Gong, M. Tong, Y. Xia, W. Cai, J. S. Moon, Y. Cao, G. Yu, C. L. Shieh, B. Nilsson, and A. J. Heeger, Science **325**, 1665 (2009).
[10]G. Li, V. Shrotriya, J. Huang, Y. Yao, T. Moriarty, K. Emery, and Y. Yang, Nat. Mater. **4**, 864 (2005).
[11]C. M. Yang, P. Y. Tsai, S. F. Horng, K. C. Lee, S. R. Tseng, H. F. Meng, J. T. Shy, and C. F. Shu, Appl. Phys. Lett. **92**, 083504 (2008).
[12]S. Cook, H. Ohkita, Y. Kim, J. J. B. Smith, D. D. C. Bradley, and J. R. Durrant, Chem. Phys. Lett. **445**, 276 (2007).
[13]Y. Kim, S. Cook, S. M. Tuladhar, S. A. Choulis, J. Nelson, J. R. Durrant, D. D. C. Bradley, M. Giles, I. Mcculloch, C. S. Ha, and M. Ree, Nat. Mater. **5**, 197 (2006).
[14]C. H. Chen and H. F. Meng, Appl. Phys. Lett. **86**, 201102 (2005).
[15]M. J. Tsai and H. F. Meng, J. Appl. Phys. **97**, 114502 (2005).
[16]Y. X. Wang, S. R. Tseng, H. F. Meng, K. C. Lee, C. H. Liu, and S. F. Horng, Appl. Phys. Lett. **93**, 133501 (2008).